International Journal of Nanomedicine

Dovepress

open access to scientific and medical research

Open Access Full Text Article

ORIGINAL RESEARCH

# Mucosal Penetrative Polymeric Micelle Formulations for Insulin Delivery to the Respiratory Tract

Ji-Hyun Kang[1,2,*], Jin-Hyuk Jeong[1,*], Yong-Bin Kwon[1], Young-Jin Kim[1], Dae Hwan Shin[1], Yun-Sang Park[3], Soonsil Hyun[1], Dong-Wook Kim[4], Chun-Woong Park[1]

[1]College of Pharmacy, Chungbuk National University, Cheongju, 28160, Republic of Korea; [2]School of Pharmacy, Institute of New Drug Development, and Respiratory Drug Development Research Institute, Jeonbuk National University, Jeonju, Republic of Korea; [3]Research & Development Center, P2K Bio, Cheongju, Republic of Korea; [4]College of Pharmacy, Wonkwang University, Iksan, 54538, Republic of Korea

*These authors contributed equally to this work

Correspondence: Chun-Woong Park, College of Pharmacy, Chungbuk National University, Cheongju, 28160, Republic of Korea, Tel +82-43-261-3330, Fax +82-43-268-2732, Email cwpark@cbnu.ac.kr; Dong-Wook Kim, College of Pharmacy, Wonkwang University, Iksan, 54538, Republic of Korea, Tel +82-63-229-7130, Fax +82-63-850-7309, Email pharmengin@gmail.com

**Purpose:** Effective mucosal delivery of drugs continues to pose a significant challenge owing to the formidable barrier presented by the respiratory tract mucus, which efficiently traps and clears foreign particulates. The surface characteristics of micelles dictate their ability to penetrate the respiratory tract mucus. In this study, polymeric micelles loaded with insulin (INS) were modified using mucus-penetrative polymers.

**Methods:** We prepared and compared polyethylene glycol (PEG)-coated micelles with micelles where cell-penetrating peptide (CPP) is conjugated to PEG. Systematic investigations of the physicochemical and aerosolization properties, performance, in vitro release, mucus and cell penetration, lung function, and pharmacokinetics/pharmacodynamics (PK/PD) of polymeric micelles were performed to evaluate their interaction with the respiratory tract.

**Results:** The nano-micelles, with a particle size of <100 nm, exhibited a sustained-release profile. Interestingly, PEG-coated micelles exhibited higher diffusion and deeper penetration across the mucus layer. In addition, CPP-modified micelles showed enhanced in vitro cell penetration. Finally, in the PK/PD studies, the micellar solution demonstrated higher maximum concentration ($C_{max}$) and $AUC_{0\text{-}8h}$ values than subcutaneously administered INS solution, along with a sustained blood glucose-lowering effect that lasted for more than 8 h.

**Conclusion:** This study proposes the use of mucus-penetrating micelle formulations as prospective inhalation nano-carriers capable of efficiently transporting peptides to the respiratory tract.

**Keywords:** insulin, polyethylene glycol, cell-penetrating peptide, aerodynamic properties, mucus penetration

## Introduction

The pulmonary administration of proteins or peptides has the potential to enhance the quality of life of patients who regularly receive needle-based injections of these therapeutic macromolecules.[1,2] Inhalation is considered a promising noninvasive route for the systemic delivery of biopharmaceuticals because of the unique characteristics of the respiratory system, such as a large absorption area, abundant blood supply, and absence of hepatic first-pass metabolism, leading to higher bioavailability compared to other noninvasive routes.[3,4] Overcoming the major physiological barriers is crucial for effective lung protein delivery. The first challenge involves penetrating the protective mucus layer of the lungs, followed by crossing the epithelial cell layer to enter the bloodstream. The second hurdle is presented by the alveoli, where the drug must evade macrophage clearance.[1,2]

Mucus and epithelial cell layers play vital roles in respiratory tract absorption by acting as protective barriers against the entry of foreign particles.[3,4] The ongoing mucus secretion serves as an effective mechanism for the entrapment of pathogens and foreign particles, thereby swiftly preventing their penetration through the epithelial barrier.[5–8] Overcoming

Received: 19 June 2024
Accepted: 28 August 2024
Published: 7 September 2024

the mucus barrier involves the development of mucus-penetrating particle carriers to prevent adherence to the mucus barrier and avoid rapid mucus clearance mechanisms.[9,10] Cutting-edge technology demonstrates that coating particles with polyethylene glycol (PEG) can create a hydrophilic and neutral surface charge, reduce mucin adsorption, and significantly improve particle transport within mucus.[10] Despite these advancements, current lung protein drug delivery modalities continue to face challenges such as low absorption and bioavailability.[11] We encapsulated a model protein, insulin (INS), in polymer micelles consisting of 1,2-dipalmitoyl-sn-glycero-3-phosphoethanolamine (DPPE) lipid conjugated to PEG (2000 and 5000 Da; DPPE-PEG) for potential pulmonary INS delivery.

To address the epithelial cell barrier, various absorption enhancers including surfactant-type molecules[12–15] and ionic liquids[16] have been developed to promote transport across the epithelial layer. Cell-penetrating peptides (CPPs) have garnered substantial interest in recent decades owing to their notable transduction efficiency (internalization into cellular membranes) and low cytotoxicity. The capacity of these peptide sequences to transport across cellular membranes makes them promising candidates for intracellular drug delivery. The attachment of cargo molecules to CPPs enables the penetration of intact cargo, facilitating their internalization into the cells.[17,18] The efficiency of CPP-mediated delivery relies on various parameters, such as the size of the cargo-CPP complex, nature of the CPP, and specific peptide sequence. For example, to achieve optimal endocytic uptake, the CPP-cargo complex should ideally be <200 nm.[19] Owing to their strong electrostatic interactions with negatively-charged cellular membranes, arginine-rich CPPs are easily internalized into biomembranes.[20] The delivery of large-molecule drugs using CPPs has been studied extensively. However, there is a notable gap in research regarding the in vivo and in vitro validation of mucus penetration effects before and after CPP application. Most studies have primarily focused on comparing mucus- and cell-penetrative nanocarriers in vitro[21] or confirming the efficacy of various cell-penetrative nanocarrier formulations in vivo.[22]

Such nanodrug delivery systems can significantly contribute to both improved mucosal and cellular penetration as well as enhanced stability.[9,23,24] By controlling physicochemical properties such as particle size, surface charge, hydrophilicity, and surface functionalization, stability can be effectively managed. The addition of amphiphilic substances, in conjunction with polymeric micelles, can ensure the structural robustness of the micelles, thereby increasing the stability of the encapsulated drug.[21,22] Furthermore, during aerosolization for inhalation delivery, the stability of peptides and proteins can be a major challenge for effective pulmonary delivery.[25,26] Well-designed nanocarriers can provide the structural integrity necessary for stable and uniform inhalation delivery of peptides and proteins. They can also overcome barriers such as mucosal and cellular penetration, thereby improving delivery efficiency. This approach promises increased bioavailability and enhanced therapeutic efficacy.[23,24]

In this study, we conjugated the CPP oligoarginine (R9) to DPPE-PEG (Figure 1), and then introduced the DPPE-PEG into Soluplus® micelles. An additional PEG layer was introduced to improve mucus penetration. PEGylation reduces the interaction between micelles and the mucus, facilitating drug absorption through the mucus layers. Although this modification is particularly beneficial for targeting drugs to mucosal tissues, it may still exhibit limited cell membrane penetration ability. The addition of R9 to DPPE-PEG micelles aimed to overcome cell penetration barrier. R9 facilitates the transport of micelles across cell membranes, thereby enhancing cell penetration and intracellular drug delivery. Collectively, these modifications aimed to increase the drug-delivery efficacy.

# Materials and Methods

## Materials

INS and rhodamine-B were purchased from Sigma-Aldrich (Sydney, Australia). Soluplus (Polyvinyl caprolactam-polyvinyl acetate-polyethylene glycol graft copolymer [PCL-PVAc-PEG]) was purchased from BASF (Ludwigshafen, Rhineland-Palatinate, Germany). DPPE-PEG 2k and 5k was purchased from Biopharma (Watertown, MA, USA). DPPE-PEG-CPP was synthesized using an amine-ester reaction, which is commonly used for PEGylation or peptide conjugation.[2,22] (Figure 2). The Calu-3 and A549 cell line were purchased from American Type Cell Culture Collection (ATCC, Rockville, MD, USA). Dulbecco's modified Eagle's medium (DMEM, without phenol red and L-glutamine), penicillin–streptomycin (10,000 U/mL), fetal bovine serum (FBS), phosphate-buffered saline (PBS), Hanks balanced salt solution (HBSS), and 0.25% trypsin-EDTA were purchased from Gibco® (New York, NY, USA). Transwell® cell culture inserts (0.33 cm2 polyester membrane, 0.4 μm

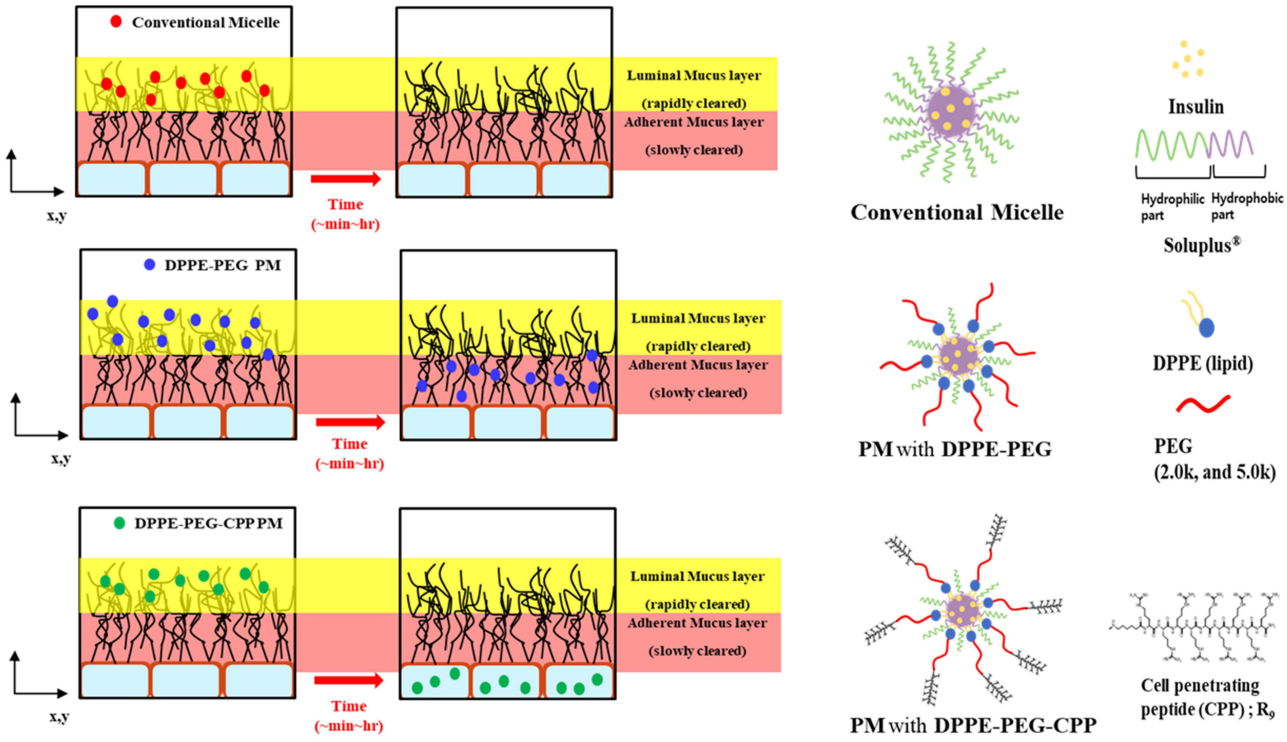


**Figure 1** Schematic representation of conventional micelles and DPPE-PEG micelles for pulmonary delivery of Insulin.

pore size) and T-75 cell culture flasks were purchased from Corning Costar® (Lowell, MA, USA). The experimental animals (8-week-old, male, Sprague-Dawley rats) were purchased from Samtaco Bio Co. (Osan, Korea). High-performance liquid chromatography (HPLC)-grade trifluoroacetic acid (TFA), ethanol, and acetonitrile (ACN) were used (Honeywell Burdick & Jackson, Muskegon, MI, USA). All other reagents were of analytical or HPLC grade.

## Preparation and Characterization of Micelles

INS (10 mg) was dissolved in 2 mL of 10 mM HCl (pH 2.0), and the pH of the solution was adjusted to 8.0 with 1 M NaOH. DPPE-PEG (10 mg; PEG MW, 2000 and 5000 Da) and 10 mg of Soluplus were dissolved in 2 mL of distilled water and added dropwise to the previously prepared INS solution (Table 1). After stirring for 1 h, the solution was purified by ultrafiltration using an Amicon® tubes (10 kDa cutoff). DPPE-PEG-CPP micelles were prepared using a same method. Rhodamine-labeled micelles were prepared using a similar method, except that rhodamine was dissolved in distilled water with DPPE-PEG. The mean particle size, size distribution, and zeta potential of the micelles were determined using a dynamic light-scattering (DLS) device (Litesizer 500; Anton Paar, Graz, Austria). Micelle morphology was evaluated by transmission electron microscopy (TEM) (JEM-2100 Plus, JEOL, Tokyo, Japan). Samples were prepared by dropping a diluted micelle suspension onto a copper grid. The samples were dried at room temperature (25 °C) for 12 h and examined. Circular dichroism (CD) spectra of INS and micelles over a wavelength range of 190–260 nm were collected using a Chirascan spectrometer (Applied Photophysics, Leatherhead, UK). The results of the encapsulation efficiency (EE, %) analysis, performed using HPLC, are expressed as the mean ± standard deviation of three independent experiments. The HPLC system (Ultimate 3000 series, Thermo Fisher Scientific, Waltham, MA, USA) was operated at 214 nm with a C18 150 * 4.60 mm, 3 μm column (Phenomenex, Torrance, CA, USA). The HPLC analysis involved a mobile phase consisting of (A) 0.1% TFA in water, and (B) 0.1% TFA in ACN at different proportions over time. The gradient was programmed as follows: from 0 to 3 min, 75% A; from 3 to 3.5 min, 20% A; and from 3.5 to 4.5 min, 75% A. Samples were eluted at a flow rate of 0.5 mL/min. The column temperature was maintained at 25 °C, and the volume of each injected sample was 20 μL. The EE% was calculated as follows:

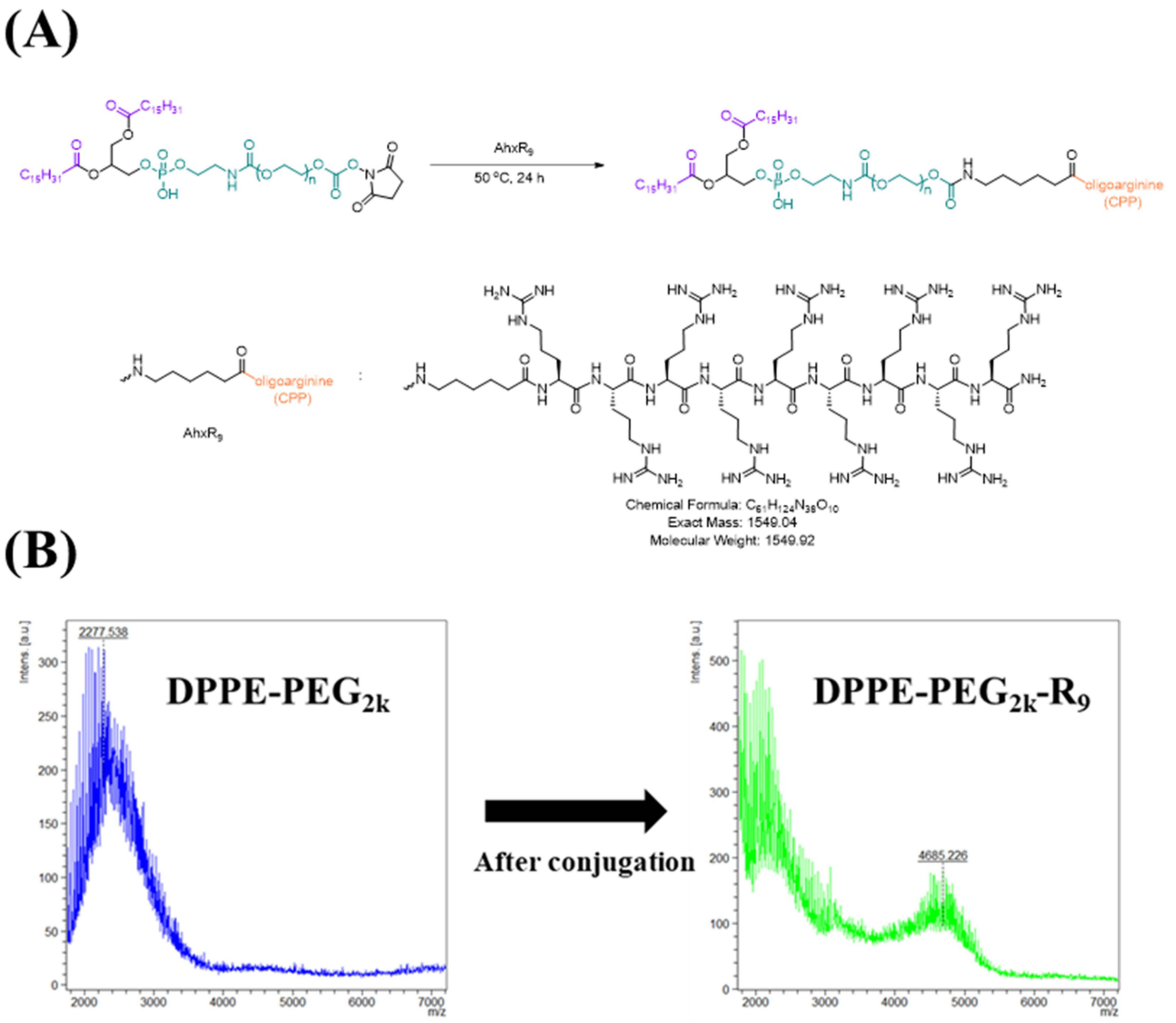


**Figure 2** (**A**) Schematic representation of R9 conjugation to the DPPE-PEG, (**B**) Mass spectrum before and after conjugation of DPPE-$PEG_{2k}$ with oligoarginine.

## In vitro Aerosol Performance

The aerosolization properties of the micelle solutions were tested in vitro using a Next Generation Impactor™ (NGI) with NGI cooler (Copley Scientific, Nottingham, UK). The NGI was coupled with a DFM critical flow controller (Copley Scientific) connected to a vacuum pump (Erweka, Langen, Germany). HPLC was used to quantify the amount of INS deposited in the NGI cups. Micelle solutions were administered using a PARI Velox® (PARI GmbH, Starnberg,

**Table 1** Formulation of the Insulin-Loaded Polymeric Micelles

| Component | PM | PEG2k | PEG5k | CPP2k | CPP5k |
|---|---|---|---|---|---|
| Insulin (INS) | 1.74 μM | 1.74 μM | 1.74 μM | 1.74 μM | 1.74 μM |
| DPPE-PEG(2.0k) | – | 3.71 μM | – | – | – |
| DPPE-PEG(5.0k) | – | – | 1.76 μM | – | – |
| DPPE-PEG(2.0k)-R9 | – | – | – | 2.35 μM | – |
| DPPE-PEG(5.0k)-R9 | – | – | – | – | 1.38 μM |
| Soluplus® | 0.08 μM | 0.08 μM | 0.08 μM | 0.08 μM | 0.08 μM |

Germany) nebulizer. The utilization of the PARI Velox nebulizer demonstrated effective nebulization of micelle solution, maintaining their structural integrity, as confirmed by particle size distribution results and observations through the PIV system (Figure S1). Briefly, 1 mL of INS solution or INS-loaded micelle solution was transferred to the reservoir, and the nebulizer was connected to the induction port of the NGI. Operating at 5 °C, at a flow rate of 15 L/min, the NGI drew the aerosol through the micro-orifice collector (MOC) with an inserted filter until complete dryness was achieved. Quantitatively recovered INS from the seven NGI collection cups was dissolved in distilled water (5 mL/cup from Stage 1 to MOC). The amount of INS deposited at the induction port was assessed by washing with an appropriate volume of water. The fine particle fraction (FPF) and geometric standard deviation (GSD) was calculated as follows:

$$\text{FPF} = (\text{mass of the particle in S3 to S7 and MOC}) \,/\, (\text{mass of the particle in all stages}) \times 100$$

$$\text{GSD} = \sqrt{(D_{84.13\%}/D_{15.87\%})}$$

$D_{84.13\%}$ and $D_{15.87\%}$ represent the diameters of the cumulative aerosol masses at 84.13% and 15.87%, respectively.

## In vitro Release Study

The release profile of INS from the micelles in vitro was examined using membrane dialysis in simulated interstitial lung fluid (SILF). Briefly, 1 L SILF contained 6.019 g sodium chloride, 0.095 g magnesium chloride, 0.298 g potassium chloride, 0.063 g sodium sulfate, 0.126 g sodium phosphate dibasic, 0.368 g calcium chloride dihydrate, 2.604 g sodium bicarbonate, 0.574 g sodium acetate, and 0.097 g sodium citrate dihydrate. INS-loaded micelles (1 mL) were placed in a dialysis bag (MWCO cutoff, 20 kDa) and submerged in 900 mL release medium at 37 °C on a shaker (200 rpm; SW22, JULABO GmbH, Seelbach, Germany). At specific time intervals, 100 µL of the micelle suspension in dialysis membrane was withdrawn and replaced with distilled water. The collected samples were subjected to HPLC analysis to determine the INS content. Each experiment was conducted in triplicates.

## Diffusion Behavior of Micelles in Mucus from Porcine Lung

Mucus was harvested from bronchoalveolar lavage fluid (BALF) collected from porcine lungs. To obtain BALF, five consecutive cycles of lung lavage were performed with the filling and emptying of the lungs with pre-warmed PBS at 37 °C. BALF was collected and centrifuged at 7500 rpm for 10 min, and the supernatant was removed to isolate the intact mucus. The isolated mucus was stored at 4 °C and used within 24 h of collection. Rhodamine-labeled micelles in mucus were tracked using multiple particle tracking (MPT) as described previously.[9–11] Specifically, 5 µL of rhodamine-labeled micelles was added to 150 µL of porcine lung mucus and vortexed for 10 min prior to microscopy. The sample was then dropped onto a cover glass and particle tracking was performed using an inverted fluorescence microscope. Video images were captured for 20s at a temporal resolution of 70 ms. Tracking videos were analyzed using the Tracker video analysis software. The coordinates of the particle centroids were transformed into time-averaged mean-squared displacement (MSD), calculated as follows:

$$\Delta r^2(\tau) = [x(t+\tau) - x(\tau)]^2 + [y(t+\tau) - y(\tau)]^2$$

where x(t) and y(t) represent the particle coordinates at a given time and t is the time scale or time lag.

## Diffusion Behavior of Micelles in Mucus from Calu-3 Cells

To assess the diffusion behavior between micelles and mucus from Calu-3 cells, the mucus penetration ability of the micelle formulations was investigated using Calu-3 cells cultured in monolayer in Transwell chambers. After equilibrating with pre-warmed HBSS for 30 min, the differentiated Calu-3 cell monolayer was exposed to rhodamine-labeled micelles for 1, 2, and 4 h at 37 °C. The cells were then washed three times with cold HBSS, fixed with 4% paraformaldehyde (PFA), stained with 50 µL of Alexa Fluor 488-labeled wheat germ agglutinin (10 µg/mL), and observed by confocal laser scanning microscopy (CLSM).

## In vitro Cell Penetration Study of Micelles Using Calu-3 and A549 Cells

Prior to the cell penetration experiment, the medium in the apical and basolateral chambers was discarded, and the cells were equilibrated with pre-warmed HBSS for 30 min at 37 °C. For quantitative analysis using HPLC, 0.2 mL of micelles with rhodamine (5 μM in HBSS) and 1.5 mL of HBSS were added to the apical and basolateral chambers of the Transwell, respectively. After incubation for 4 h at 37 °C, the cells were washed three times with cold HBSS. For qualitative analysis using CLSM, 0.2 mL of rhodamine-labeled micelle solution and 1.5 mL of HBSS were added to the apical and basolateral chambers, respectively. After incubation for 4 h at 37 °C, the cells were washed three times with cold HBSS, fixed with 4% PFA, stained with Hoechst 33342 (Sigma-Aldrich, Darmstadt, Germany), and observed by CLSM.

## Pharmacokinetic Study

All animal experiments were conducted in accordance with the "Principles of Laboratory Animal Care" and approved by the Committee for the Institutional Animal Care and Use Committee of the Chungbuk National University.

Male Sprague-Dawley (SD) rats weighing 220–240 g (Samtako) were used for the experiments. The rats were fed a commercial pellet diet, provided with freshwater, and housed at 23 ± 1 °C with relative humidity of 50 ± 10%, and a 12-hour light and dark cycle. The animals were randomly divided into five groups: INS solution administered subcutaneously (S.C) or via intra-tracheal instillation (I.T.I) and micellar formulations (PM, PEG2k, and CPP2k) administered via I.T.I. The INS solution and micelle formulations were administered at a concentration of 10 IU/kg. The rats were anesthetized using isoflurane, and 500 μL of blood was collected from the retro-orbital sinus in heparin tubes, followed by centrifugation (5 min, 2000 rpm) to obtain plasma. The plasma was analyzed immediately after collection using an INS ELISA Kit (Eagle Biosciences, Amherst, NH, USA).

## Pharmacodynamic Studies

Male SD rats weighing 220–240 g were used for the experiments. To establish a streptozotocin (STZ)-induced diabetic rat model, the rats were intraperitoneally injected 60 mg/kg STZ. After the first injection, diabetic rats with blood glucose levels >300 mg/dL were selected for further in vivo testing. Blood was collected from the tail of the rats, and glucose levels were analyzed using an Accu-Chek Performa® (Roche, Basel, Switzerland) glucometer. The animals were randomly divided into six groups: NC (saline-treated, negative control), INS solution administered via S.C. and I.T.I routes, and PM, PEG2k, and CPP2k micelle formulations administered via I.T.I. The INS solution and micelle formulations were administered at a concentration of 5 IU/kg.

## Statistical Analyses

All statistical analyses were conducted using the Kruskal–Wallis test and performed using GraphPad Prism 8 (version 8.4.2; San Diego, CA, USA). The p-values are reported in the corresponding figure legends. Statistical significance was set at $p < 0.05$.

# Results and Discussion

## Properties and Characteristics of Micelles

DLS analysis confirmed that the micelles achieved diameters of approximately <100 nm through self-assembly. As shown in Figure 3A, the micelles exhibited a size range of 65–85 nm with a low particle distribution index. The sizes of PM, PEG2k, PEG5k, CPP2k, and CPP5k micelles were 65.74 ± 0.35, 71.75 ± 1.08, 74.37 ± 0.50, 93.37 ± 2.89, and 94.60 ± 1.14 nm, respectively. Mucus secretions have been reported to exhibit a wide mesh size distribution, with the average mesh size ranging between 140 and 340 nm. Therefore, the <100 nm size would allow for easy diffusion of the micelles through the mucus.[9] Additionally, analysis of the micelles before and after nebulization using the PARI Velox nebulizer confirmed that the size of micelles remained unchanged, indicating the stability of the micellar structures (Figure S1). As shown in Figure 3B, the EE% for INS in PM, PEG2k, PEG5k, CPP2k, and CPP5k micelles were 46.05 ± 1.06%, 61.93 ± 1.66%, 62.17 ± 1.53%, 68.08 ± 5.45%, and 67.33 ± 1.04%, respectively. The amphiphilic properties of Soluplus are thought to facilitate the encapsulation of the hydrophilic compound INS within micelles. The EE% was higher in lipid-PEG and lipid-PEG-CPP than PM. The addition of lipid-PEG to micelles made with Soluplus enhanced the EE% of INS owing to its unique properties. Lipid-PEG is amphiphilic

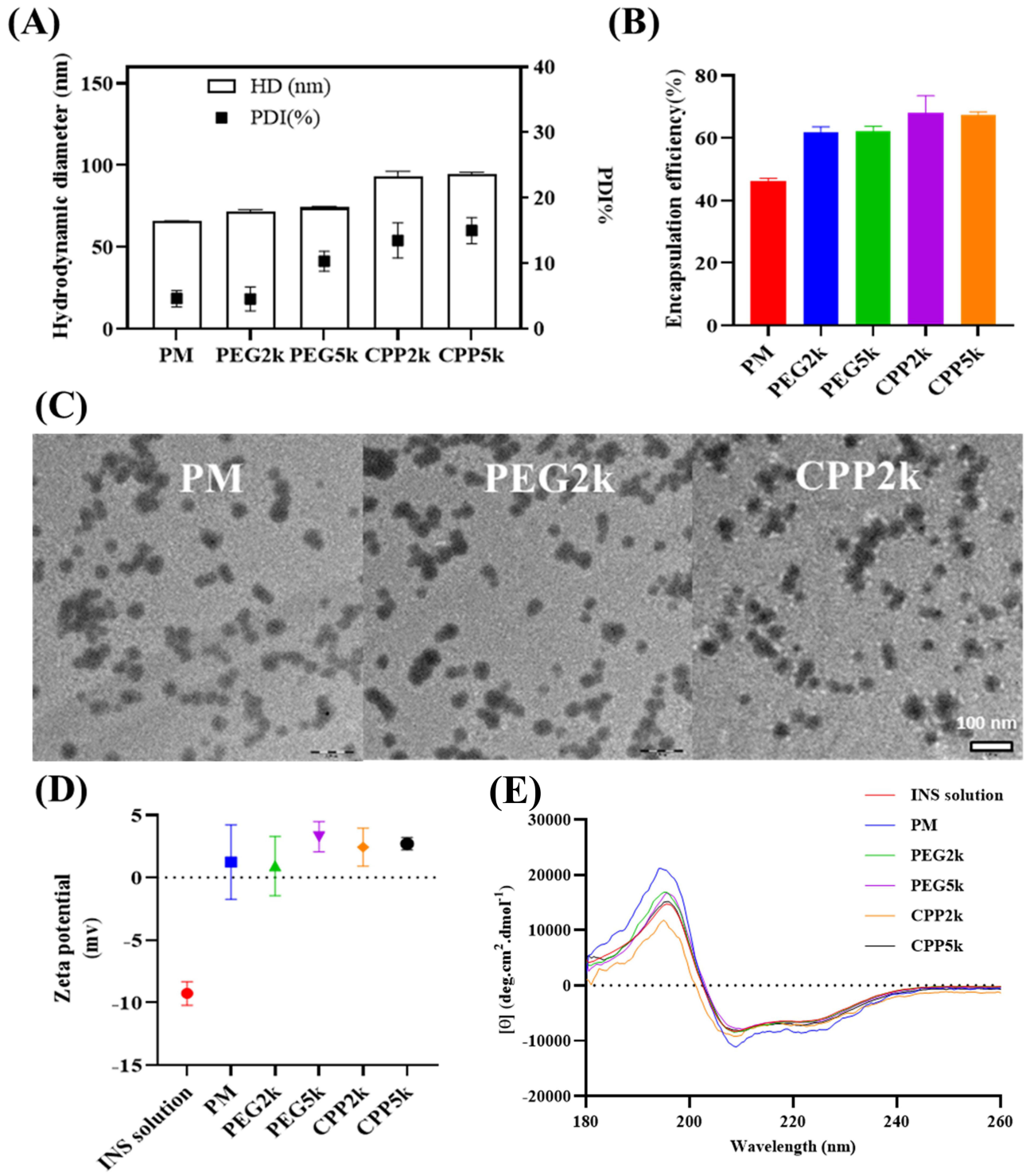


**Figure 3** (**A**) Hydrodynamic diameter and PDI of the micelle formulations, (**B**) Encapsulation efficiency, (**C**) Transmission electron microscopic (TEM) images of the micelle formulations (Scale bar = 100 nm), (**D**) zeta potential, and (**E**) CD spectrum. Each value represents the mean ± standard deviation (n = 3).

and possesses both hydrophobic and hydrophilic components. The lipid-PEG component interacts with both the hydrophobic core of the micelle and the hydrophilic environment, thereby facilitating the encapsulation of INS molecules. The hydrophobic portion of lipid-PEG integrates with the hydrophobic domains of Soluplus micelles, contributing to the stability and structure of the micellar system. Simultaneously, the hydrophilic PEG segment provides a protective shell around the micelles, preventing

aggregation and enhancing solubility in aqueous environment.[21,22] This dual interaction capability of lipid-PEG helps accommodate INS molecules more efficiently within the micellar structure, leading to an increase in the EE. The enhanced encapsulation results in higher protection of INS and improved bioavailability, making the micellar system with Soluplus and lipid-PEG a more effective carrier for INS delivery. As shown in Figure 3C, TEM images of the micelles showed a typical spherical morphology with a particle size of approximately <50 nm, which is smaller than the hydrodynamic diameter because of the PEG chains on the micelle surface. The INS-loaded micelles showed a neutral zeta potential compared to that of the INS solution (−9.6 mV), indicating successful INS encapsulation and stability of INS micelles with a nearly neutral potential (Figure 3D). In all micelle formulations, the zeta potential appears to be determined by the Soluplus. This is because Soluplus has a very high molecular weight of approximately 120,000 g/mol and has more charges per molecule compared to PEG or PEG-CPP. Negatively-charged particles are rapidly opsonized and extensively cleared by fixed macrophages of the reticuloendothelial system (RES) in the bloodstream.[23] Surface modification of nanodrug delivery systems is the most common strategy for controlling opsonization, so as to sustain these systems for a longer period in the bloodstream.[23,24] Owing to the shielding effect induced by the amphiphilic polymers and lipid-PEG or lipid-PEG-CPP, the zeta potential of the micelles decreased. The reduced zeta potential of these micelles also suggests potentially advantageous pharmacokinetics for in vivo applications, such as increased half-life and bioavailability.[24] Additionally, as shown in Figure 3E, CD spectrum analysis confirmed that the micelle formulations displayed the same signals as native INS, indicating that the secondary structure and bioactivity of INS remained unchanged.

## In vitro Aerosol Performance

The effective delivery of an inhaled medication relies on its deposition pattern within the respiratory system through a process that is influenced by various factors, including formulation properties, inhaler device characteristics, and individual physiological attributes. Particles with mass median aerodynamic diameter (MMAD) <5 μm are generally presumed to be deposited in the lungs, whereas those with MMADs <3 μm can reach the alveoli, thereby facilitating local therapeutic effects or potential systemic absorption. Prior research has established a satisfactory correlation between in vitro particle size and aerosolization profiles and the in vivo deposition pattern in the lungs.[25] The necessity for in vitro data on the particle size distribution and aerosolization properties of inhalable formulations by regulatory agencies stems from the need to assess formulation efficiency prior to approval. Consequently, the FPF, representing the percentage of particles <5 μm in the total emitted dose (ED) that can effectively reach and deposit in the airways and deep lung, serves as a key indicator in this evaluation process. The deposition profile of aerosol formulations in the lungs is directly linked to both their pharmacological efficacy and clinical outcomes; thus, higher amounts of INS are expected to reach the lungs and become available for absorption with PM, PEG2k, and CPP2k formulations than with the INS solution. Nonetheless, INS bioavailability is not solely contingent on its deposition profile. Consequently, a higher FPF does not necessarily equate to elevated therapeutic efficacy. This complexity makes it challenging to compare formulations based solely on their in vitro deposition profiles. In practice, even if the particles reach deep lungs, the realization of significant therapeutic effects is contingent on the effective release of INS from the formulations and/or its absorption through the epithelium. The deposition ratio (%) of INS at each stage is shown in Figure 4A, and the aerosol performance parameters are listed in Table 2. Based on the FPF% <5.39 μm, no significant differences were observed between the INS solution and micelle formulations (PM, PEG2k, and CPP2k). However, when considering the FPF% <3.30 μm, PEG2k and CPP2k exhibited significantly higher values than the INS solution (Figure 4B). The FPF values <3.3 μm for INS solution, PM, PEG2k, and CPP2k micelles were 64.32 ± 5.62%, 77.82 ± 1.82%, 83.24 ± 5.66%, and 85.95 ± 3.46%, respectively and their MMAD values were measured as 5.58 ± 1.48, 4.36 ± 1.33, 3.64 ± 1.11, and 3.38 ±0.99 μm, respectively. This suggests that the micelles provide a protective environment for INS, preventing its aggregation or degradation during aerosolization.[26] This could have resulted in a more uniform distribution of INS in the aerosol, thus contributing to a higher FPF%. Therefore, the additional components (lipid-PEG and lipid-PEG-CPP) contributed to the stability of the micelles. A stable micellar structure is crucial for maintaining the integrity of the formulation during nebulization, which can positively impact aerosol performance. Incorporating a hydrophilic polymer (PEG) into the outer shells of PEG2k and CPP2k resulted in repulsive steric interactions among the droplets. This effectively reduces the overall adhesive force, facilitating more efficient aerosolization and enhancing the stability of the colloidal suspensions in air.[26–29]

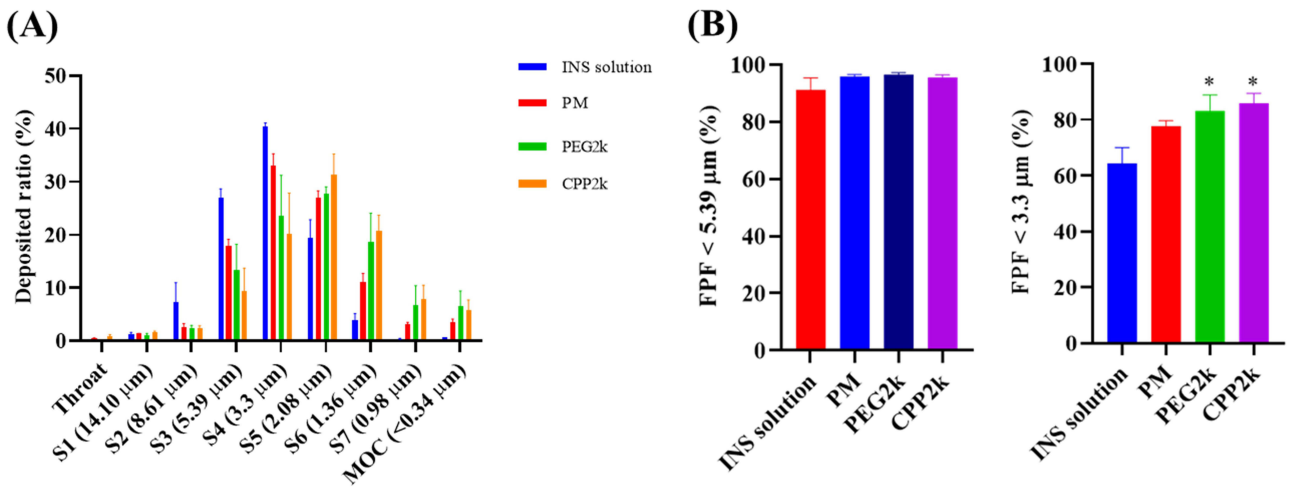


**Figure 4** (**A**) Aerosol dispersion performance as percentage deposited in each stage of NGI, (**B**) FPF (%) below 5.39 and 3.30 μm of each formulation (mean ± standard deviation, n = 3). *Significantly different from INS solution ($p < 0.05$, Kruskal–Wallis test).

## In vitro Release

As shown in Figure 5, PM, PEG2k, and CPP2k demonstrated a sustained-release profile with a cumulative release of only approximately 40% during the same period. These findings suggest that micelles based on INS not only efficiently encapsulate the drug but also achieve sustained release of INS. The sustained-release behavior of the micelles, likely attributable to the slower diffusion of INS from the micelles, could prevent the dispersion of INS across the respiratory tract fluid before its efficient penetration into micelles through the mucus, thus facilitating effective drug delivery.[30] Additionally, this sustained-release profile is advantageous for drug delivery applications, offering a more controlled and prolonged therapeutic effect. The ability of the micelle formulation to provide sustained drug release may be attributed to factors such as improved drug encapsulation within the micellar core, optimized drug solubility, and modulation of release kinetics through the micelle structure. Overall, the sustained-release profile observed in this study underscores the potential of Soluplus and lipid-PEG micelle formulations as promising candidates for controlled-drug delivery applications.

## Diffusion Behavior of Micelles in Mucus from Porcine Lung

To incorporate surface characteristics that are both hydrophilic and electrically neutral, our strategy involved coating the particles with hydrophilic yet uncharged polymers. PEG is a suitable candidate for this purpose as it is an uncharged and highly flexible polymer commonly employed in the field of drug delivery.[31,32] Additionally, PEG-grafted nanoparticles are known to effectively prolong systemic circulation times effectively,[33,34] making them a suitable choice for minimizing adhesive interactions with mucins. Mucus barriers along the mucosal epithelia play a critical role in swiftly entrapping and removing the majority of external nanoparticles within the mucosal environment, potentially compromising the effectiveness of nanocarrier-based drug delivery.[35] Enhancing the efficacy of mucosal delivery requires nano-carriers with the capability of rapid mobility and diffusion through protective mucus linings.[36] Consequently, evaluating the diffusion behavior within

**Table 2** Aerosol Performance Characteristics Including FPF, MMAD, and GSD of Insulin Solution and Micelle Formulations

| Component | INS solution | PM | PEG2k | CPP2k |
|---|---|---|---|---|
| $FPF_{< 5.39\ \mu m}$ (%) | 91.33 ± 4.03 | 95.74 ± 0.77 | 96.51 ± 0.73 | 95.45 ± 1.04 |
| $FPF_{< 3.3\ \mu m}$ (%) | 64.32 ± 5.62 | 77.82 ± 1.82* | 83.24 ± 5.66* | 85.95 ± 3.46* |
| MMAD (μm) | 5.58 ± 1.48 | 4.36 ± 1.33 | 3.64 ± 1.11 | 3.38 ± 0.99 |
| GSD | 1.57 ± 0.02 | 1.75 ± 0.06 | 1.85 ± 0.05 | 1.77 ± 0.08 |

**Notes**: Data are presented as mean ± standard deviation (n = 3) *Significantly different from INS solution ($p < 0.05$, Kruskal–Wallis test).

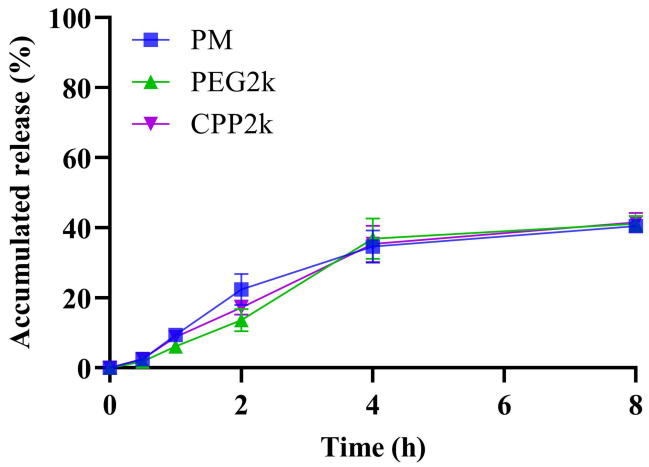


**Figure 5** In vitro release profile of insulin in simulated interstitial lung fluid (SILF). Each value represents the mean ± standard deviation (n = 3).

respiratory mucus is crucial for assessing the penetrability of nano-carriers. Furthermore, exploring diffusion in mucus can offer supportive insights into the effectiveness of the surface coatings in mitigating interactions with mucus. The transport dynamics of micelles in porcine respiratory mucus were investigated using MPT. As shown in Figure 6A, PM exhibited highly hindered trajectories and was nearly immobilized in the mucus. In contrast, the PEG-coated micelles (PEG2k, PEG5k, CPP2k, and CPP5k) were mobilized to greater distances and were more diffusive. The MSD of the PEG-coated micelles was markedly greater than that of PM (Figure 6B). At 1 s, the MSD of the PEG-coated micelles was approximately 100-fold greater than that of the PM. The results demonstrated that the PEG-coated micelles exhibited unconstrained movement in the mucus compared to the PM. Therefore, faster diffusion of PEG-coated micelles in mucus is beneficial for improving mucus penetration efficiency. Since there was no significant difference between PEG2K and PEG5K regardless of the presence of CPP, only PEG2K and CPP2K formulations were evaluated in the subsequent tests.

## Diffusion Behavior of Micelles in Mucus from Calu-3 Cells

The diffusion of rhodamine-loaded micelles into the mucus of Calu-3 cells was monitored using CLSM imaging. When cultured at the air-liquid interface (ALI), Calu-3 cells serve as a human bronchial cell model capable of mucus production. This mucus layer provides a suitable platform for investigating particle penetration.[37] Control cells exhibited a green-labeled mucus layer characterized by dense areas of a fibrous network at the top, with interspersed loose regions believed to contain interstitial fluid.[38] After incubation for 4 h, PEG2k and CPP2k exhibited significantly greater red fluorescence in the mucus layer than PM (Figure 7A), indicating that the PEG-coated micelles moved faster in mucus than PM. To enable a quantitative comparison of the extent of micelle diffusion in the Calu-3 cell mucus, the fluorescence intensity of each micelle sample at different time points was

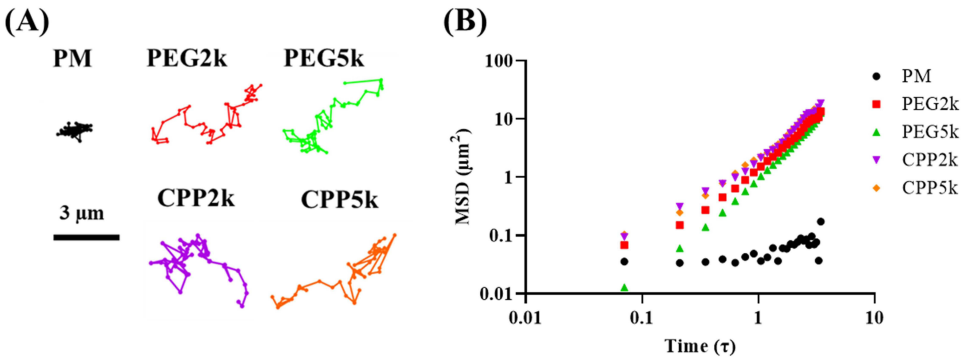


**Figure 6** (**A**) Representative trajectories of the micelle in mucus; (**B**) Ensemble-averaged geometric mean squared displacement (MSD) as a function of timescale for micelle in mucus. Each value represents the mean ± standard deviation (n = 3).

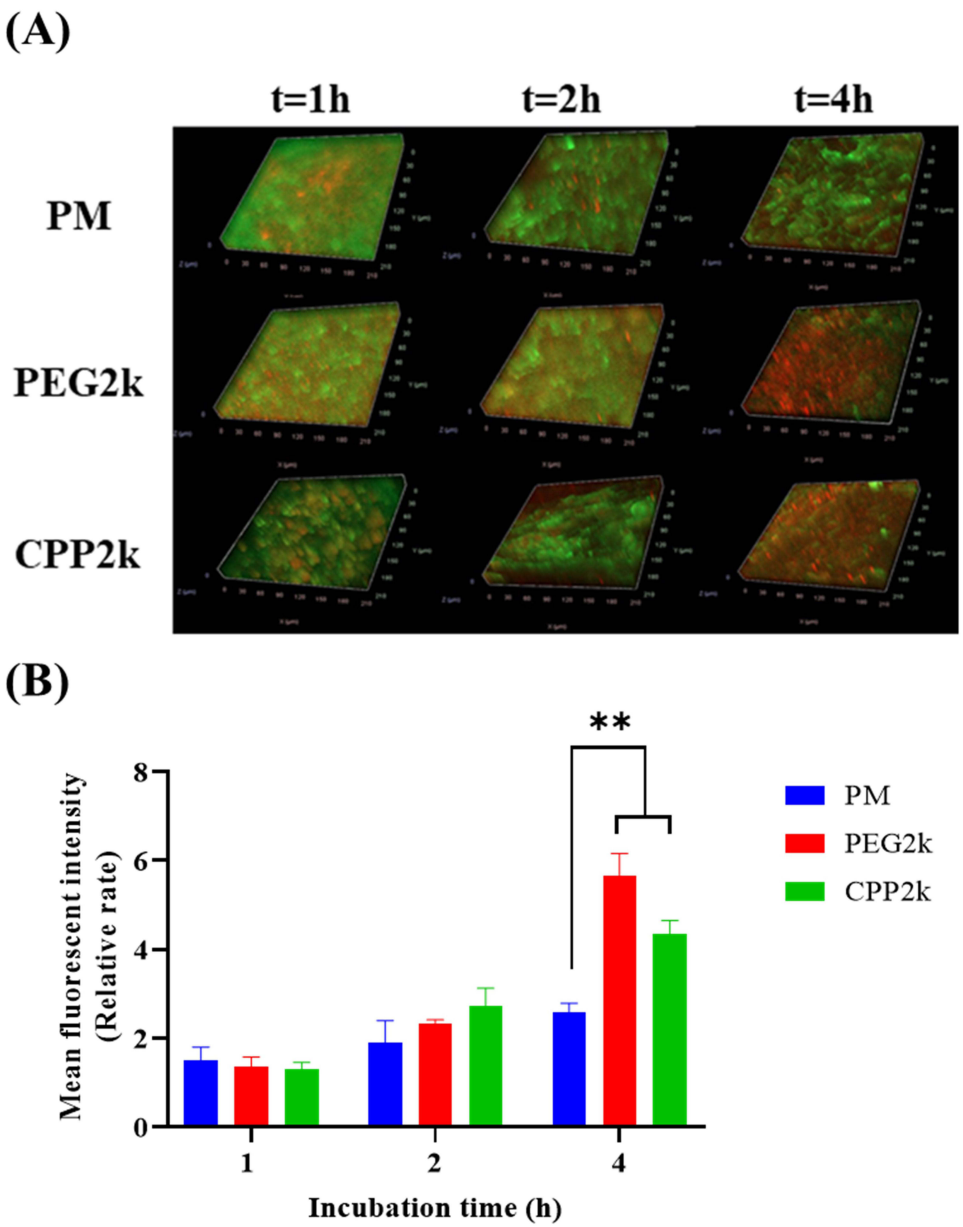


**Figure 7** (**A**) Z-stacks of particle diffusion (red) in mucus as a function of time, and (**B**) Mean fluorescent intensity of PM, PEG2k, and CPP2k. Each value represents the mean ± standard deviation (n = 3). **Significantly different from PM ($p < 0.01$, Kruskal–Wallis test).

analyzed using image analysis software. The fluorescence intensities of PEG2k and CPP2k after 4 h were significantly higher than those of PM (Figure 7B). PEG2k and CPP2k appear to be more efficient than PM in micelle diffusion in mucus. PEG is highly hydrophilic, which helps prevent strong adhesive interactions with the hydrophobic mucin proteins present in the mucus. This reduces the tendency of micelles to adhere to the mucus layer, allowing for smoother diffusion. In addition, the assessment of cell viability using the MTT assay provided valuable insights into the safety profile of the INS solution and micelle formulations (Figure S2). These findings contribute to the overall understanding of the biocompatibility of micelle delivery systems and support their potential as safe and viable platforms for peptide drug delivery in future applications.

## In vitro Cell Penetration Studies Using A549 and Calu-3 Cells

Achieving effective cell penetration of large biologically active molecules poses a considerable challenge to drug design and controlled-drug delivery. Over the past few years, a multitude of interdisciplinary research endeavors have highlighted diverse

applications of CPPs in transporting various payloads, including nucleic acids, polymers, liposomes, nanoparticles, and low-molecular-weight drugs.[39] We investigated the permeability of micelles using A549 and Calu-3 cells. A particularly intriguing result was the substantial improvement in cell permeability when CPP was incorporated into the micelles (CPP2k). Arginine-rich CPP use an alternative mechanism for cellular entry that bypasses direct penetration through lipid membranes. Instead, they enter vesicles and viable cells by inducing membrane multilamellae and fusion.[40] Arginine-rich peptides with distinctive cell-penetrating capabilities have garnered considerable scientific interest. Positively-charged essential amino acids enable interactions with negatively-charged drug molecules and cell membranes through non-covalent mechanisms, such as electrostatic interactions, contributing to their noteworthy properties. As shown in Figure 8, CPP2k demonstrated significantly enhanced cell permeability

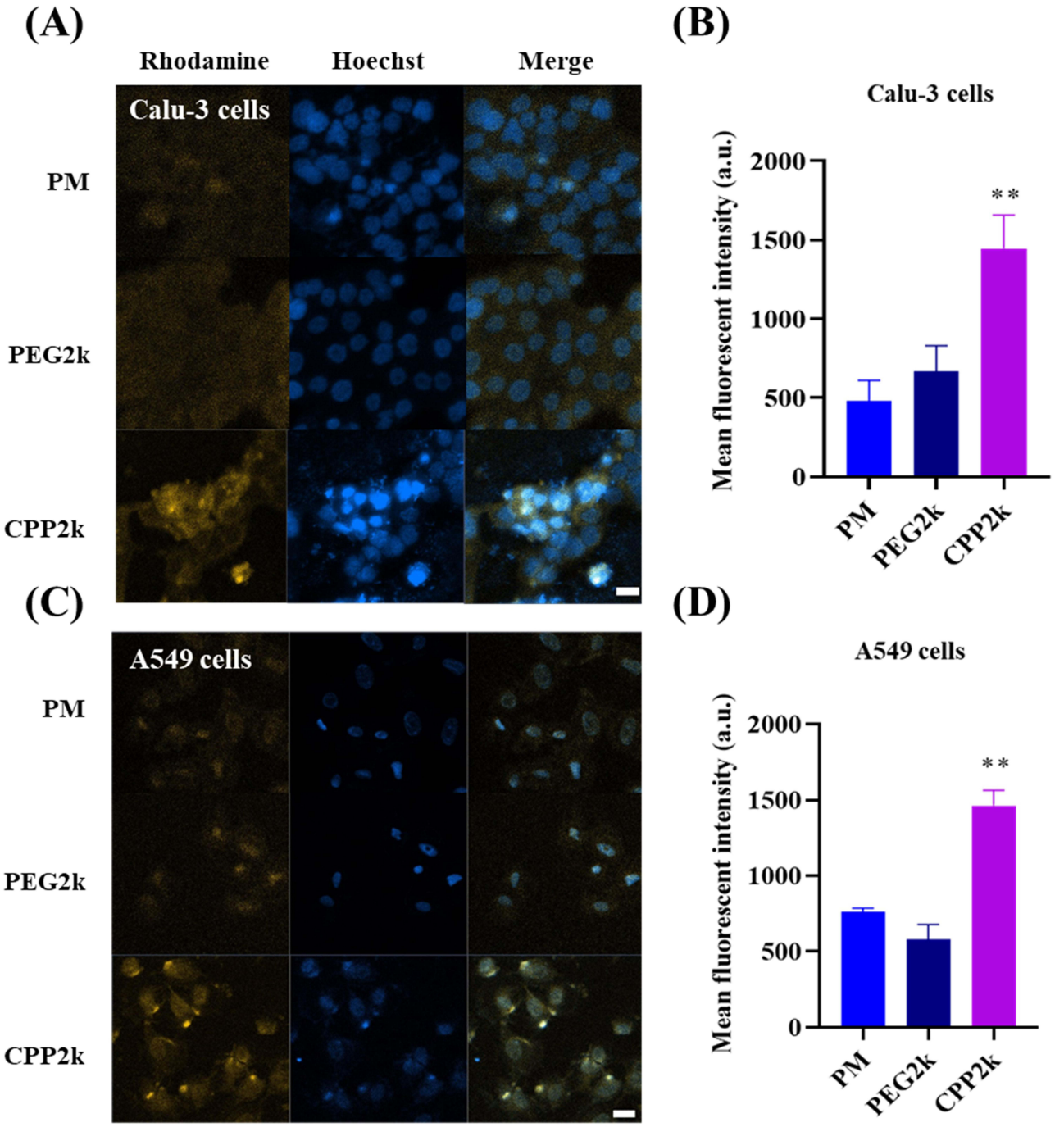


**Figure 8** (**A**) CLSM image of micelles using Calu-3 cells; (**B**) Mean fluorescent intensity results in Calu-3 cells (mean ± standard deviation, n = 3); (**C**) CLSM image of micelles using A549 cells; (**D**) Mean fluorescent intensity results in A549 cells (mean ± standard deviation, n = 3). **Significantly different from PM and PEG2k ($p < 0.01$, Kruskal–Wallis test).

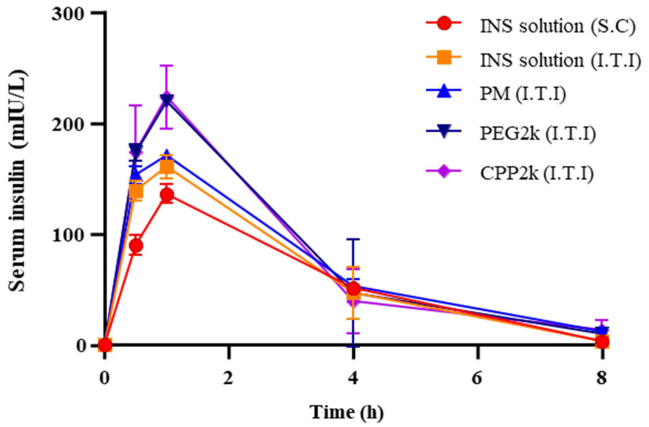


**Figure 9** Serum insulin level in non-diabetic rat administered insulin solution (via subcutaneous [S.C] and intratracheal instillation [I.T.I] route at 10 IU/kg), and different insulin-loaded formulations (PM, PEG2k, and CPP2k, 10 IU/kg) by I.T.I (mean ± standard deviation, n = 4).

compared to PM and PEG2k. These findings suggest that surface modification of micelles with CPP improves cell permeability.[41] The internalization phenomenon remains unexplained by conventional endocytosis mechanisms because major inhibitors of endocytosis and metabolism have proven to be ineffective. No substantial disruption of the cell membranes was observed. Additionally, Suzuki et al indicated that the interaction of these peptides may involve cell-surface-sulfated polysaccharides.[42] However, the mechanism by which these peptides traverse the cell membrane remains elusive, particularly after potential adsorption to the external surface of the plasma membrane via sulfated polysaccharides. The conventional energy-dependent endocytosis pathway, specifically clathrin-coated pit-mediated endocytosis,[43] does not appear to be the predominant route for internalization, as evidenced by the limited impact of various endocytosis and metabolic inhibitors on uptake. Recently, Eguchi et al reported that a λ phage expressed the basic domain of the Tat protein on its surface internalized into mammalian cells via the caveolae-mediated pathway.[44] Therefore, caveolae-mediated endocytosis may be involved in the internalization of arginine-rich peptides. These discoveries serve as crucial indicators for the development of nano-carriers with high efficiency in future applications in drug delivery. The ability to modulate cell permeability through surface modifications, particularly CPP, opens up new avenues for designing nano-carriers that can more effectively navigate cellular barriers, leading to improved therapeutic outcomes of various drug delivery systems.

## Pharmacokinetic Study

Analyses of the pharmacokinetic profile (Figure 9) provided insights into the comparative effects of S.C and I.T.I routes of administration of INS solution at a dose of 10 IU/kg. Both routes of administration led to a rapid increase in INS concentration within the first hour. Interestingly, despite the same dose being administered, I.T.I resulted in a higher INS concentration profile than S.C route. This suggests that administering INS directly into the lungs results in higher bioavailability and a more potent pharmacological effect than S.C injection. Similarly, micellar solutions (PM, PEG2k, and CPP2k) administered by I.T.I also resulted in a rapid increase in INS concentration within the initial stage. The pharmacokinetic parameters at 10 IU/kg are presented in Table 3. Notably, the area under the curve ($AUC_{0\text{-}8h}$) for the

**Table 3** Pharmacokinetic Parameters of INS and Micelle Solutions Following Administration by Subcutaneous Injection (S.C) or Intratracheal Instillation (I.T.I)

| Formulation | Route | Dose (IU/kg) | $C_{max}$ (mL/L) | $AUC_{0-8h}$ (mIU/L*h) |
|---|---|---|---|---|
| INS solution | S.C. | 10 | 136.5 ± 9.181 | 471.2 ± 8.971 |
| INS solution | I.T.I. | 10 | 160.9 ± 10.60 | 521.2 ± 88.96 |
| PM | I.T.I. | 10 | 170.8 ± 0.992 | 584.6 ± 23.48 |
| PEG2k | I.T.I. | 10 | 220.6 ± 1.483*** | 646.8 ± 176.5 |
| CPP2k | I.T.I. | 10 | 223.6 ± 28.48*** | 643.2 ± 26.01* |

**Notes**: Data are presented as mean ± standard deviation (n = 4). *$p < 0.05$, ***$p < 0.001$, significantly different from INS solution administrated by S.C., Kruskal–Wallis test.

CPP2k micelle solution was significantly higher (643.2 ± 26.01 mIU/L*h) than that for INS solution S.C (471.2 ± 8.97 mIU/L*h). Although there was no significant difference in the $AUC_{0\text{-}8h}$ between the PM and INS solutions, PEG2k and CPP2k demonstrated higher AUC. Owing to the sustained release of micelles and increased mucus and cell penetration abilities, the bioavailability increases.[45] The enhanced bioavailability of micelle formulations may potentially improve therapeutic efficacy. PEG2k and CPP2k yielded similar results. This is attributed to the fact that the barrier posed by mucus during pulmonary drug delivery is greater than that of cellular penetration in normal lung.[46,47] These findings underscore the significance of micelle delivery systems in influencing the pharmacokinetics of peptide drugs and support their application as a promising platform for optimized drug delivery.

## Pharmacodynamic Study

In this study, we used the STZ-induced diabetic rats because they have been acknowledged as a reliable animal model for evaluating novel formulations designed for INS delivery.[48] In this diabetic rat model, INS and micelle solutions were administered at a concentration of 2 IU/kg via two routes: S.C and I.T.I. Unlike approaches involving nose-only or whole-body ventilation chambers in certain inhalation studies, the I.T.I technique requires a smaller sample volume and specifically targets the distal regions of the lungs. This is achieved by delivering the formulations near the carina, bypassing the mouth and trachea.[49] Encapsulation of peptides for inhalation has been reported as a strategy to enhance their bioavailability, protect them from degradation, and augment their transepithelial transport.[50] The therapeutic effect of inhaled formulations designed for the systemic delivery of peptides involves an equilibrium encompassing the deposition profile within the respiratory system, liberation from the formulation, potential degradation, macrophage uptake, elimination by defense mechanisms, and absorption into the bloodstream. In this study, using double-chamber plethysmography, we concluded that there were no changes in lung function following the administration of a single dose of the INS-loaded micelles (Figure S3), indicating their safety. As shown in Figure 10, at 2 h post-administration, both PEG2k and CPP2k formulations resulted in a significant reduction in blood glucose levels compared to the standard INS solution administered by S.C and I.T.I routes. The blood glucose levels for INS solution administrated by S.C and I.T.I, and that of PM, PEG2k, and CPP2k formulations were 333.7 ± 46.48 mg/dL, 303.3 ± 14.29 mg/dL, 313.67 ± 36.56 mg/dL, 162.3 ± 27.54 mg/dL, and 147.67 ± 33.56 mg/dL, respectively. In vitro research has shown that polymers with intermediate-length PEG blocks and lipophilicity exhibit greater interference with the membrane,[51] potentially contributing to increased permeation. However, no significant difference in the hypoglycemic effect was observed between the PEG2k and CPP2k formulations. The mucus layer may impede the diffusion of INS molecules, thereby preventing them from reaching the cell membrane. The restricted movement of PM in the mucus layer likely leads to its entrapment

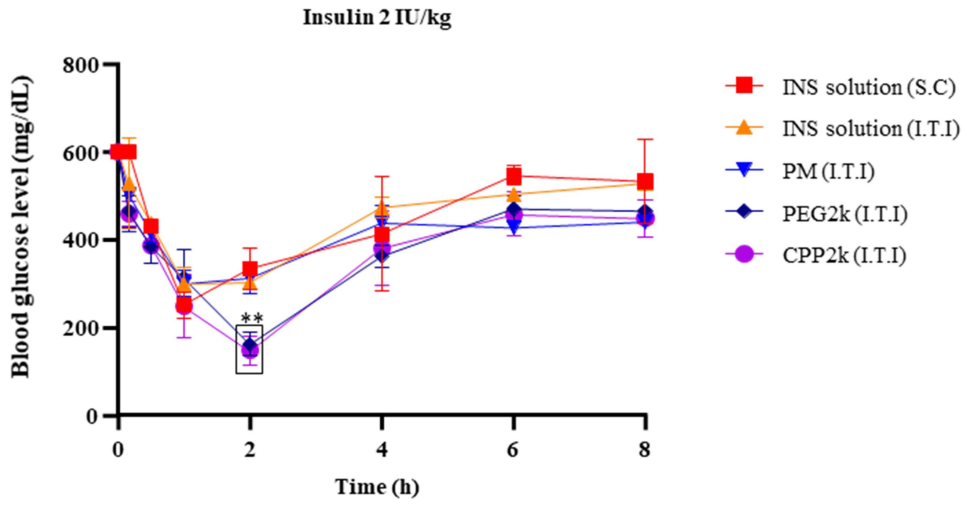


**Figure 10** Blood glucose level in diabetic rat administered insulin (S.C or I.T.I, 2 IU/kg), normal saline, and different insulin-loaded formulations (PM, PEG2k, and CPP2k) by I.T.I (mean ± standard deviation, n = 4). **Significantly different from INS solution (S.C and I.T.I) and PM ($p < 0.01$, Kruskal–Wallis test).

within the mucus and subsequent removal via mucociliary clearance.[52,53] In contrast, PEGylated PEG2k and CPP2k are hypothesized to traverse the mucus layer more rapidly because of their PEG modifications. However, beyond the mucus layer, there was no significant difference in the ability of PEG2k and CPP2k to permeate the cell membrane in vivo, which was consistent with the observed lack of significant variation in their hypoglycemic effects. This suggests that the rate of mucus penetration, rather than the subsequent cell membrane permeation, may be a key determinant of the efficacy of these inhalable peptide drug formulations.

## Conclusion

In this study, we comprehensively evaluated surface-functionalized polymeric micelles, specifically those designed for mucus penetration. Collectively, our findings suggest promising outcomes for the administration of peptide drugs through mucus-penetrative micelles via inhalation. The rapid drug diffusion observed in freshly obtained porcine and Calu-3 cell mucus indicated the effectiveness of both the micelle (PEG2k and CPP2k) formulations in facilitating improved drug penetration through the mucus layer. This enhanced penetration translated into superior in vitro cell penetration in Calu-3 and A549 cells when CPP-based micelles were used, indicating their potential for enhanced bioavailability and cellular targeting. An in vivo PK study confirmed that the inhalation route was more effective for peptide drug delivery compared with S.C injection and that both the mucus-penetrative micelles formulations were more effective than conventional polymeric micelles. The higher $AUC_{0\text{-}8h}$ of both the micelle solutions further support the notion that surface-functionalized micelles enhance the therapeutic efficacy of peptide drug delivery. The results of the in vitro experiments suggest that CPP2k has superior bioavailability compared to PEG2k. However, no difference in AUC between the two micelles were observed in the in vivo PK studies. These results indicate that under normal pulmonary conditions, mucus penetration serves as a more significant barrier than cellular penetration during pulmonary administration. Overcoming this barrier can significantly enhance the bioavailability of peptide drugs. In conclusion, this study positions mucus-penetrative micelle formulations as prospective inhalation nano-carriers capable of efficiently transporting peptides to the respiratory tract.

## Data Sharing Statement

The data will be available from the corresponding author.

## Funding

This study was supported by the National Research Foundation of Korea grants provided by the Korean government (NRF-2021R1A2C4002746 and 2017R1A5A2015541). This study was supported by the Regional Innovation Strategy (RIS) through the National Research Foundation of Korea (NRF), funded by the Ministry of Education (MOE) (2021RIS-001). Following are results of a study on the "Leaders in INdustry-university Cooperation 3.0" Project, supported by the Ministry of Education and National Research Foundation of Korea.

## Disclosure

The authors report no conflicts of interest in this work.

## References

1. Yang MS, Kang JH, Kim DW, Park CW. Recent developments in dry powder inhalation (DPI) formulations for lung-targeted drug delivery. *J Pharm Investig*. 2023;54(2):1–18. doi:10.1007/s40005-023-00635-w
2. Perry JL, Reuter KG, Kai MP, et al. PEGylated PRINT nanoparticles: The impact of PEG density on protein binding, macrophage association, biodistribution, and pharmacokinetics. *Nano Lett*. 2012;12(10):5304–5310. doi:10.1021/nl302638g
3. Cu Y, Saltzman WM. Mathematical modeling of molecular diffusion through mucus. *Adv Drug Deliv Rev*. 2009;61(2):101–114. doi:10.1016/j.addr.2008.09.006
4. Saltzman WM, Radomsky ML, Whaley KJ, Cone RA. Antibody diffusion in human cervical mucus. *Biophys J*. 1994;66(2):508–515. doi:10.1016/S0006-3495(94)80802-1
5. Chilvers MA, O'callaghan C. Local mucociliary defence mechanisms. *Paediatr Respir Rev*. 2000;1(1):27–34. doi:10.1053/prrv.2000.0009
6. Knowles MR, Boucher RC. Mucus clearance as a primary innate defense mechanism for mammalian airways. *J Clin Invest*. 2002;109(5):571–577. doi:10.1172/JCI0215217

7. McAuley JL, Linden SK, Png CW, et al. MUC1 cell surface mucin is a critical element of the mucosal barrier to infection. *J Clin Invest*. 2007;117(8):2313–2324. doi:10.1172/JCI26705
8. Cone RA. Barrier properties of mucus. *Adv Drug Deliv Rev*. 2009;61(2):75–85. doi:10.1016/j.addr.2008.09.008
9. Yu T, Choi WJ, Anonuevo A, et al. Mucus-penetrating nanosuspensions for enhanced delivery of poorly soluble drugs to mucosal surfaces. *Adv Healthc Mater*. 2016;5(21):2745. doi:10.1002/adhm.201600599
10. Lai SK, O'Hanlon DE, Harrold S, et al. Rapid transport of large polymeric nanoparticles in fresh undiluted human mucus. *Proc Natl Acad Sci*. 2007;104(5):1482–1487. doi:10.1073/pnas.0608611104
11. Lewis SA, Berg JR, Kleine TJ. Modulation of epithelial permeability by extracellular macromolecules. *Physiol Rev*. 1995;75(3):561–589. doi:10.1152/physrev.1995.75.3.561
12. McCartney F, Gleeson JP, Brayden DJ. Safety concerns over the use of intestinal permeation enhancers: A mini-review. *Tissue Barriers*. 2016;4(2):e1176822. doi:10.1080/21688370.2016.1176822
13. Maher S, Mrsny RJ, Brayden DJ. Intestinal permeation enhancers for oral peptide delivery. *Adv Drug Deliv Rev*. 2016;106(Pt B):277–319. doi:10.1016/j.addr.2016.06.005
14. Whitehead K, Karr N, Mitragotri S. Safe and effective permeation enhancers for oral drug delivery. *Pharm Res*. 2008;25(8):1782–1788. doi:10.1007/s11095-007-9488-9
15. Kapitza C, Zijlstra E, Heinemann L, Castelli MC, Riley G, Heise T. Oral insulin: A comparison with subcutaneous regular human insulin in patients with type 2 diabetes. *Diabetes Care*. 2010;33(6):1288–1290. doi:10.2337/dc09-1807
16. Noh G, Keum T, Bashyal S, et al. Recent progress in hydrophobic ion-pairing and lipid-based drug delivery systems for enhanced oral delivery of biopharmaceuticals. *J Pharm Investig*. 2022; 2022:1–19. doi:10.1007/s40005-021-00549-5
17. Prochiantz A. Messenger proteins: homeoproteins, TAT and others. *Curr Opin Cell Biol*. 2000;12(4):400–406. doi:10.1016/S0955-0674(00)00108-3
18. Guidotti G, Brambilla L, Rossi D. Cell-penetrating peptides: From basic research to clinics. *Trends Pharmacol Sci*. 2017;38(4):406–424. doi:10.1016/j.tips.2017.01.003
19. Thapa RK, Kim JO. Nanomedicine-based commercial formulations: Current developments and future prospects. *J Pharm Investig*. 2023;53(1):19–33. doi:10.1007/s40005-022-00607-6
20. El Andaloussi S, Lehto T, Mäger I, et al. Design of a peptide-based vector, PepFect6, for efficient delivery of siRNA in cell culture and systemically *in vivo*. *Nucleic Acids Res*. 2011;39(9):3972–3987. doi:10.1093/nar/gkq1299
21. Porsio B, Craparo EF, Mauro N, Giammona G, Cavallaro G. Mucus and cell-penetrating nanoparticles embedded in nano-into-micro formulations for pulmonary delivery of ivacaftor in patients with cystic fibrosis. *ACS Appl Mater Interfaces*. 2018;10(1):165–181. doi:10.1021/acsami.7b14992
22. Osman G, Rodriguez J, Chan SY, et al. PEGylated enhanced cell penetrating peptide nanoparticles for lung gene therapy. *J Control Release*. 2018;285:35–45. doi:10.1016/j.jconrel.2018.07.001
23. Martin AR, Finlay WH. Nebulizers for drug delivery to the lungs. *Expert Opin Drug Deliv*. 2015;12(6):889–900. doi:10.1517/17425247.2015.995087
24. Honary S, Zahir F. Effect of zeta potential on the properties of nano-drug delivery systems-a review (Part 2). *Trop J Pharm Res*. 2013;12(2):265–273. doi:10.4314/tjpr.v12i2.20
25. Xin X, Chen J, Chen L, Wang J, Liu X, Chen F. Lyophilized insulin micelles for long-term storage and regulation of blood glucose for preventing hypoglycemia. *Chem ENG J*. 2022;435:134929. doi:10.1016/j.cej.2022.134929
26. Fröhlich E, Salar-Behzadi S. Oral inhalation for delivery of proteins and peptides to the lungs. *Eur J Pharm Biopharm*. 2021;163:198–211. doi:10.1016/j.ejpb.2021.04.003
27. Newman SP, Chan HK. *In vitro*/*in vivo* comparisons in pulmonary drug delivery. *J Aerosol Med Pulm Drug Deliv*. 2008;21(1):77–84. doi:10.1089/jamp.2007.0643
28. Yamamoto H, Kuno Y, Sugimoto S, Takeuchi H, Kawashima Y. Surface-modified PLGA nanosphere with chitosan improved pulmonary delivery of calcitonin by mucoadhesion and opening of the intercellular tight junctions. *J Control Release*. 2005;102(2):373–381. doi:10.1016/j.jconrel.2004.10.010
29. Dailey LA, Schmehl T, Gessler T, et al. Nebulization of biodegradable nanoparticles: Impact of nebulizer technology and nanoparticle characteristics on aerosol features. *J Control Release*. 2003;86(1):131–144. doi:10.1016/S0168-3659(02)00370-X
30. Coombes AGA, Tasker S, Lindblad M, et al. Biodegradable polymeric microparticles for drug delivery and vaccine formulation: The surface attachment of hydrophilic species using the concept of poly (ethylene glycol) anchoring segments. *Biomater*. 1997;18(17):1153–1161. doi:10.1016/S0142-9612(97)00051-3
31. Dong W, Ye J, Zhou J, et al. Comparative study of mucoadhesive and mucus-penetrative nanoparticles based on phospholipid complex to overcome the mucus barrier for inhaled delivery of baicalein. *Acta Pharm Sin B*. 2020;10(8):1576–1585. doi:10.1016/j.apsb.2019.10.002
32. Zhu M, Nie G, Meng H, Xia T, Nel A, Zhao Y. Physicochemical properties determine nanomaterial cellular uptake, transport, and fate. *Acc Chem Res*. 2013;46(3):622–631. doi:10.1021/ar300031y
33. Gref R, Minamitake Y, Peracchia MT, Trubetskoy V, Torchilin V, Langer R. Biodegradable long-circulating polymeric nanospheres. *Science*. 1994;263(5153):1600–1603. doi:10.1126/science.8128245
34. Jokerst JV, Lobovkina T, Zare RN, Gambhir SS. Nanoparticle PEGylation for imaging and therapy. *Nanomedicine*. 2011;6(4):715–728. doi:10.2217/nnm.11.19
35. Amoozgar Z, Yeo Y. Recent advances in stealth coating of nanoparticle drug delivery systems. *Wiley Interdiscip Rev Nanomed Nanobiotechnol*. 2012;4(2):219–233. doi:10.1002/wnan.1157
36. Yu T, Chan KW, Anonuevo A, et al. Liposome-based mucus-penetrating particles (MPP) for mucosal theranostics: Demonstration of diamagnetic chemical exchange saturation transfer (diaCEST) magnetic resonance imaging (MRI). *Nanomedicine*. 2015;11(2):401–405. doi:10.1016/j.nano.2014.09.019
37. Mura S, Hillaireau H, Nicolas J, et al. Biodegradable nanoparticles meet the bronchial airway barrier: How surface properties affect their interaction with mucus and epithelial cells. *Biomacromolecules*. 2011;12(11):4136–4143. doi:10.1021/bm201226x
38. Lai SK, Wang YY, Wirtz D, Hanes J. Micro-and macrorheology of mucus. *Adv Drug Deliv Rev*. 2009;61(2):86–100. doi:10.1016/j.addr.2008.09.012
39. Langel Ü eds. *Cell-Penetrating Peptides*. Vol. 683. Totowa, New Jersey: Humana Press; 2011. doi:10.1007/978-1-60761-919-2

40. Allolio C, Magarkar A, Jurkiewicz P, et al. Arginine-rich cell-penetrating peptides induce membrane multilamellarity and subsequently enter via formation of a fusion pore. *Proc Natl Acad Sci USA*. 2018;115(47):11923–11928. doi:10.1073/pnas.1811520115
41. Futaki S, Suzuki T, Ohashi W, et al. Arginine-rich peptides: an abundant source of membrane-permeable peptides having potential as carriers for intracellular protein delivery. *J Biol Chem*. 2001;276(8):5836–5840. doi:10.1074/jbc.M007540200
42. Suzuki T, Futaki S, Niwa M, Tanaka S, Ueda K, Sugiura Y. Possible existence of common internalization mechanisms among arginine-rich peptides. *J Biol Chem*. 2002;277(4):2437–2443. doi:10.1074/jbc.M110017200
43. Mukherjee S, Ghosh RN, Maxfield FR. Endocytosis. *Physiol Rev*. 1997;77(3):759–803. doi:10.1152/physrev.1997.77.3.759
44. Eguchi A, Akuta T, Okuyama H, et al. Protein transduction domain of HIV-1 Tat protein promotes efficient delivery of DNA into mammalian cells. *J Biol Chem*. 2001;276(28):26204–26210. doi:10.1074/jbc.M010625200
45. Shan W, Zhu X, Liu M, et al. Overcoming the diffusion barrier of mucus and absorption barrier of epithelium by self-assembled nanoparticles for oral delivery of insulin. *ACS Nano*. 2015;9(3):2345–2356. doi:10.1021/acsnano.5b00028
46. Chen D, Liu J, Wu J, Suk JS. Enhancing nanoparticle penetration through airway mucus to improve drug delivery efficacy in the lung. *Expert Opin Drug Deliv*. 2021;18(5):595–606. doi:10.1080/17425247.2021.1854222
47. Nguyen J, Xie X, Neu M, et al. Effects of cell-penetrating peptides and pegylation on transfection efficiency of polyethylenimine in mouse lungs. *J Gene Med*. 2008;10(11):1236–1246. doi:10.1002/jgm.1255
48. King AJ. The use of animal models in diabetes research. *Br J Pharmacol*. 2012;166(3):877–894. doi:10.1111/j.1476-5381.2012.01911.x
49. Helms MN, Torres-Gonzalez E, Goodson P, Rojas M. Direct tracheal instillation of solutes into mouse lung. *J Vis Exp*. 2010;42:e1941. doi:10.3791/1941
50. Andrade F, Videira M, Ferreira D, Sarmento B. Nanocarriers for pulmonary administration of peptides and therapeutic proteins. *Nanomedicine*. 2011;6(1):123–141. doi:10.2217/nnm.10.143
51. Batrakova EV, Li S, Alakhov VY, Miller DW, Kabanov AV. Optimal structure requirements for pluronic block copolymers in modifying P-glycoprotein drug efflux transporter activity in bovine brain microvessel endothelial cells. *J Pharmacol Exp Ther*. 2003;304(2):845–854. doi:10.1124/jpet.102.043307
52. Bustamante-Marin XM, Ostrowski LE. Cilia and mucociliary clearance. *Cold Spring Harb Perspect Biol*. 2017;9(4):a028241. doi:10.1101/cshperspect.a028241
53. Yue WL. Nasal mucociliary clearance in patients with diabetes mellitus. *J Laryngol Otol*. 1989;103(9):853–855. doi:10.1017/S0022215100110291